

Superconductivity from a pseudogapped normal state: a mode coupling approach to precursor superconductivity

Jiri Maly, Boldizsár Jankó, and K. Levin

The James Franck Institute, The University of Chicago, 5640 S. Ellis Avenue, Chicago IL 60637
(November 20, 2016)

We derive a phase diagram for the pseudogap onset temperature T^* (associated with the breakdown of the Fermi liquid state, due to strong pairing correlations) and the superconducting instability, T_c , as a function of variable pairing strength. Our diagrammatic approach to the BCS - Bose-Einstein cross-over problem self consistently treats the coupling between the single particle and pair propagators, and leads to a continuous evolution of these propagators into the standard $T < T_c$ counterparts. A rich structure is found in T_c which reflects the way in which the superconducting instability at T_c is affected by the pseudogap Δ_{pg} . An important consequence of Cooper-pair-induced pseudogaps is that the magnitude of T_c is sustained, even when $\Delta_{pg} > T_c$.

PACS numbers: 74.20.Mn, 74.25.-q, 74.25.Fy, 74.25.Nf, 74.72.-h

It is generally agreed that the pseudogap state of the underdoped cuprates represents some type of pairing above T_c which is postulated to derive from neutral spinon pairs [1], spin [2] or charge [3] density wave states, or from some form of ($2e$) Cooper pairing which foreshadows the ultimate superconducting state. Each of these scenarios must not only address the nature of the exotic (ie., pseudogapped) normal state but also the transition from this state to its associated superconducting instability. Indeed, there is an extensive literature on the problem of establishing superconductivity in the presence of gaps in the electronic spectral function [4]. In this paper we investigate this issue under the presumption that the normal state spectral function gap is associated with Cooper pairing above T_c . Moreover, by self-consistently coupling the single particle and pair properties we establish the nature and physics of the pseudogap state. In this coupled scheme, we demonstrate how gapping in the electronic spectrum affects T_c and argue that this $2e$ pairing is not particularly deleterious to the superconductivity, despite the relatively large size of the pseudogap ($\Delta_{pg} > T_c$). Our results are consolidated into a phase diagram in which the pseudogap phase occupies a large temperature range in the limit of moderately strong superconducting coupling.

An important contribution of this paper is to revisit the BCS - Bose Einstein cross-over problem [5] using a conserving diagrammatic “mode coupling” formulation. Above T_c this approach leads to one and two electron Green’s functions which are formally continuous with their below T_c counterparts obtained in the standard theory of superconductivity. This approach also reproduces the expected limits associated with the extreme weak and strong coupling regimes of previous saddle point schemes [6]. The intermediate coupling regime is of particular importance to the cuprates and Monte Carlo simulations [7] suggest that deviations from Fermi liquid behavior are present there. Our previous diagrammatic calculations [8] indicate that long lived pairs introduce a gap

in the electronic spectral function by blocking available single particle states around the Fermi surface. This gap correlates with a regime of *resonant* pair scattering which forms a natural intermediate state between the free fermions of the weak coupling, and the composite bosons of the strong coupling limits. In the present fully self consistent theory, this resonant scattering will, itself, be modified by pseudogap effects.

We consider a generic Hamiltonian consisting of fermions in the presence of an attractive interaction, which may be modeled as $V_{\mathbf{k},\mathbf{k}'} = g\varphi_{\mathbf{k}}\varphi_{\mathbf{k}'}$, where $\varphi_{\mathbf{k}} = (1 + k^2/k_0^2)^{-1/2}$ and $g < 0$ is the coupling strength often expressed in units of $g_c = -4\pi/mk_0$ [9]. The BCS - Bose Einstein cross-over problem is characterized by coupled equations for T_c and the chemical potential, μ . The former derives from the Thouless criterion for the pair propagator or T-matrix, and the latter from the particle number equation, which involves the single particle propagator. In general, the full treatment of the coupling between the pair and single particle propagators is referred to as “mode coupling”. In the present formulation the coupled equations are obtained following earlier literature on superconducting fluctuation effects [10]

$$\Sigma_{\mathbf{k},i\omega_l} = T \sum_{\mathbf{q},\Omega_m} t_{\mathbf{q},i\Omega_m} G_{\mathbf{q}-\mathbf{k},i\Omega_m-i\omega_l}^{(0)} \varphi_{\mathbf{k}-\mathbf{q}/2}^2, \quad (1)$$

$$t_{\mathbf{q},i\Omega_m}^{-1} = g^{-1} + T \sum_{\mathbf{k},\omega_l} G_{\mathbf{k},i\omega_l} G_{\mathbf{q}-\mathbf{k},i\Omega_m-i\omega_l}^{(0)} \varphi_{\mathbf{k}-\mathbf{q}/2}^2. \quad (2)$$

where the Green’s function is given by $G_{\mathbf{k},i\omega_l}^{-1} = G_{\mathbf{k},i\omega_l}^{(0)-1} - \Sigma_{\mathbf{k},i\omega_l}$, $G_{\mathbf{k},i\omega_l}^{(0)-1} = i\omega_l - \epsilon_{\mathbf{k}}$, Ω_m/ω_l are the even/odd Matsubara frequencies, and the electronic dispersion is $\epsilon_{\mathbf{k}} = k^2/2m - \mu$.

At high temperatures where mode coupling or “feedback effects” may be ignored [8], all Green’s functions in Eqs. 1 and 2 may be replaced by bare propagators. If we restrict our attention to moderately strong coupling constants, $g/g_c \sim 1$ (associated with $k_F\xi/2\pi \sim 1-10$), we find a Fermi liquid phase above a crossover temperature

T^* . The break-down of the Fermi liquid at $T_{\text{Res}} \sim T^*$ coincides with the onset of resonant pair scattering. As the temperature is lowered below T^* the gap in the spectral function grows as the resonant states become more long lived. Finally, at T_c , coherent pairs condense into a superconducting ground state. The value of T_c is obtained by solving Eqs. 1 and 2, which, at T_c , become

$$\Sigma_{\mathbf{k},\omega} = -\Delta_{\text{pg}}^2 \varphi_{\mathbf{k}}^2 G_{\mathbf{k},-\omega}^{(0)}, \quad (3)$$

$$t_{\mathbf{0},0}^{-1} = g^{-1} + \sum_{\mathbf{k}} \frac{1 - 2f(E_{\mathbf{k}})}{2E_{\mathbf{k}}} \varphi_{\mathbf{k}}^2. \quad (4)$$

where $E_{\mathbf{k}} = \sqrt{\epsilon_{\mathbf{k}}^2 + \Delta_{\text{pg}}^2 \varphi_{\mathbf{k}}^2}$. The pseudogap parameter is, at arbitrary temperatures, defined to be

$$\Delta_{\text{pg}}^2 = \sum_{\mathbf{q}} \int_{-\infty}^{\infty} \frac{d\Omega}{\pi} b(\Omega) \text{Im} t_{\mathbf{q},\Omega}, \quad (5)$$

where $f(\omega), b(\omega) = (\exp(\omega/T) \pm 1)^{-1}$. It is evident that Δ_{pg}^2 in Eq. 5 coincides with the square amplitude of pairing fluctuations, $g^2 < c^\dagger c^\dagger c c >$.

It should be noted that Eqs. 3 and 4 provide an important validation for the diagrammatic scheme of Eqs. 1 and 2. These two equations show that a pseudogap in the normal state spectrum preserves the overall ‘‘BCS-like’’ structure of the T_c equation as well as the diagonal component of the single particle Green’s functions. This continuity implies that, even though these equations are derived above T_c , they are formally identical to their one and two particle counterparts of the standard superconducting state [11]. This is in contrast to the use of fully renormalized Green’s functions everywhere.

In order to evaluate T_c it is necessary to further simplify Eq. 5. As a first step, we investigate the T-matrix in the presence of a pseudogap. To capture the essential physics, we use a time dependent Ginzburg-Landau (TDGL) formulation

$$gt_{\mathbf{q},\Omega}^{-1} = \tau_0 - (a'_0 + ia''_0)\Omega + b_0\Omega^2 + \xi_{\text{LG}}^2 q^2, \quad (6)$$

where the TDGL parameters can be calculated by a formal expansion of the full T-matrix at low frequencies and momenta. For intermediate coupling and at sufficiently low Ω and \mathbf{q} , the T-matrix assumes the resonant form

$$t_{\mathbf{q},\Omega} = \frac{ga_0^{-1}}{\Omega - \Omega_{\mathbf{q}} + i\Gamma_{\mathbf{q}}}, \quad (7)$$

where a_0 is predominantly real. It follows from Eq. 2, that feedback effects, associated with a gap in the single particle spectrum, lead to a gap in the imaginary part of the inverse T-matrix at T_c . This latter gap affects $\Gamma_{\mathbf{q}}$ in an important way: when $\Omega_{\mathbf{q}} < \Delta_{\text{pg}}$, $\Gamma_{\mathbf{q}} \rightarrow 0$. This gap is slightly smeared out for temperatures between T^* and T_c , but, nevertheless $\Gamma_{\mathbf{q}}$ remains small. Thus mode coupling leads to a stabilization of resonance effects, and,

thereby an amplification of pseudogap behavior. This TDGL formulation is in contrast to results obtained from previous cross-over TDGL theories [12] which omit mode coupling, as well as from applications to dirty superconductors [10], where mode coupling is included, but gap effects are absent.

The above results can now be applied to rewrite Eq. 5 and, thereby, compute the superconducting instability temperature, T_c . The value of T_c is obtained from a solution of the Thouless condition (Eq. 4) and the number equation in the presence of the self-consistently determined pseudogap amplitude Δ_{pg} . The coupled equations for this transition temperature follow from Eqs. 3-5 and are given by

$$1 + g \sum_{\mathbf{k}} \frac{1 - 2f(E_{\mathbf{k}})}{2E_{\mathbf{k}}} \varphi_{\mathbf{k}}^2 = 0, \quad (8)$$

$$2 \sum_{\mathbf{k}} \left[v_{\mathbf{k}}^2 + \frac{\epsilon_{\mathbf{k}}}{E_{\mathbf{k}}} f(E_{\mathbf{k}}) \right] = n, \quad (9)$$

$$\sum_{\mathbf{q}}^{\Omega_{\mathbf{q}} < \Delta_{\text{pg}}} \frac{b(\Omega_{\mathbf{q}})}{\frac{\partial}{\partial \Omega} \text{Re} t_{\mathbf{q},\Omega}^{-1} \Big|_{\Omega_{\mathbf{q}}}} = \Delta_{\text{pg}}^2, \quad (10)$$

where $v_{\mathbf{k}}^2 = (1 - \epsilon_{\mathbf{k}}/E_{\mathbf{k}})/2$.

We solved Eqs. 8-10 numerically to obtain T_c as a function of g/g_c , along with the resonance onset temperature T_{Res} , which we associate with T^* . Our results are plotted in Fig. 1. Also shown (dashed line) is the superconducting instability temperature T_0 computed in the absence of mode coupling. When there is an appreciable pseudogap, T_c and T^* vary in an inverse fashion with g/g_c . This is a consequence of the pseudogap which suppresses T_c , but is not present at T^* . In this way the pseudogap regime is greatly enhanced by mode coupling contributions.

The overall behavior of T_c is compared with that obtained from the saddle point approximation, as well as that of strict BCS theory in Fig. 2(a). Here the inset plots the chemical potential and pseudogap function (at T_c), along with T_c . It can be seen from the inset, that the maximum in T_c is associated with $\mu \sim \Delta_{\text{pg}}$ and the minimum with $\mu = 0$. Indeed, the complex behavior of T_c shown in Fig. 2 can be understood on general physical grounds. A local maximum appears in the T_c curve as a consequence of a growing (with increased coupling) pseudogap Δ_{pg} in the fermionic spectrum which weakens the superconductivity. However, even as Δ_{pg} grows, superconductivity is sustained. In the present scenario, superconductivity is preserved by the conversion of an increasing fraction of fermions to bosonic states, which can then Bose condense. Once the fermionic conversion is complete ($\mu = 0$), T_c begins to increase again with coupling. This is a consequence of the decreasing pair size and concomitant reduction of the Pauli principle repulsion.

The behavior of T_c on an expanded coupling constant

scale, for different ranges of the interaction (parameterized by k_0/k_F) is shown in Fig. 2(b). The limiting value of T_c for large values of g/g_c approaches the ideal Bose-Einstein condensation temperature $T_{BE} = 0.218E_F$ as $k_0 \rightarrow \infty$ [13]. The qualitative shape of the T_c curve, however, is retained as long as k_0/k_F is greater than about 0.5. For larger range interactions, the solution disappears for some g/g_c ; then, when μ is sufficiently negative, the transition reappears approaching a continuously (with $k_0/k_F \rightarrow 0$) decreasing asymptote.

In order to implement the mode coupling scheme away from T_c , we introduce a two parameter fit to the full self-energy which is based on, and evolves smoothly into Eq. 3 at T_c ,

$$\Sigma_{\mathbf{k},\omega}^{\text{mc}} = \frac{\Delta_{\text{pg}}^2 \varphi_{\mathbf{k}}^2}{\omega + \epsilon_{\mathbf{k}} + i\gamma}. \quad (11)$$

This model makes it possible to do systematic numerics in the well established pseudogap phase, but it is not appropriate in a regime in which the pseudogap breaks down as it evolves towards the Fermi liquid state. The instability of the Fermi liquid, or pseudogap onset T^* , is, however, addressed using the lowest order expansion of Eqs. 1 and 2, as discussed above. The parameter Δ_{pg} in Eq. 11 is defined from Eq. 5, which is numerically implemented via

$$\Delta_{\text{pg}}^2 \varphi_{\mathbf{k}}^2 = - \int_{-\infty}^{\infty} \frac{d\omega}{\pi} \text{Im} \Sigma_{\mathbf{k},\omega}. \quad (12)$$

Similarly, the parameter γ is obtained from the height of the peak in $-\text{Im} \Sigma_{\mathbf{k},\omega}$ which is defined to be $\Delta_{\text{pg}}^2 \varphi_{\mathbf{k}}^2 / \gamma$. It should be stressed that at T_c the parameter γ in Eq. 11 becomes zero, as is implied by Eq. 3. This results from the continuity of the pseudogap and superconducting phases, and can be seen explicitly by noting that T_c occurs when the T-matrix becomes singular at $\Omega = 0$ and $\mathbf{q} = 0$ (the Thouless criterion). As a result, a divergent peak in $\text{Im} \Sigma_{\mathbf{k},\omega}$ occurs at $\omega = -\epsilon_{\mathbf{k}}$.

The coupled equations for $\Sigma_{\mathbf{k},\omega}$ and $t_{\mathbf{q},\Omega}^{-1}$, as a function of temperature, were solved numerically using the model self-energy of Eq. 11 and the TDGL approximation of Eq. 6. In a given iteration Δ_{pg} and γ were used to compute $t_{\mathbf{q},\Omega}$ via Eq. 2 which was then approximated by Eq. 6 for use in Eq. 1. The output of the latter was then used to extract Δ_{pg} and γ via Eq. 11 and the procedure repeated until convergence. In this way Δ_{pg} , γ , $\Omega_{\mathbf{q}}$, and $\Gamma_{\mathbf{q}}$ were all determined self-consistently as a function of temperature and coupling constant.

To emphasize the important coupling between these electronic and pair properties, we compare the evolution of the single particle parameters Δ_{pg} and γ with the pair parameters $\Omega_{\mathbf{q}=0}$ and $\Gamma_{\mathbf{q}=0}$ in Fig. 3 for $g/g_c = 1.2$. The associated spectral functions over this range of temperatures are shown by the inset in Fig. 3(a). The shaded regions indicate where the two parameter model self-energy

of Eq. 11 breaks down, as does the lowest order theory; even though the pseudogap persists, the system begins to cross-over towards the Fermi liquid. Thus the parameters Δ_{pg} and γ are indicated only for a limited range of temperatures. The temperature for Fermi liquid onset, $T_{\text{Res}} \sim T^*$, is just beyond the shaded region corresponding to the regime of validity of the lowest order theory. This temperature can be read off from the endpoint of the two curves in Fig. 3(b). Moreover, the ratio $\Delta_{\text{pg}}^2 / \gamma$ which represents the peak height of $\text{Im} \Sigma_{\mathbf{k},\omega}$, appears to extrapolate smoothly from the mode coupling results to zero at T_{Res} , at which point the Fermi liquid state sets in and $\text{Im} \Sigma_{\mathbf{k},\omega}$ changes character. As indicated in Fig. 3(a), the disappearance of the pseudogap arises via a reduction in Δ_{pg} , while the peak broadening remains relatively small. This latter is a consequence of the extended lifetime of the pairs due to a full (*s*-wave) gap in the T-matrix. This gap is also responsible for the relatively small values (when compared to conventional TDGL theory [10]) of $\Gamma_{\mathbf{q}=0}$, which is associated with the inverse pair lifetime, shown in Fig. 3(b). At higher temperatures $\Gamma_{\mathbf{q}=0}$ and $\Omega_{\mathbf{q}=0}$ are plotted to join, after extrapolation, onto the results of the lowest order theory.

In summary, within a BCS - Bose Einstein cross-over picture, we have presented a quantitative phase diagram which compares the temperature onset of the pseudogap with the onset of a novel superconducting state, associated with pseudogapped fermions. Mode coupling effects, which were important for this analysis, considerably enhance the pseudogap regime. We have demonstrated (for the *s*-wave case) that this pseudogap disappears with temperature, as it evolves into a Fermi liquid state, principally by a reduction in the gap size Δ_{pg} . While we have not established detailed connections to the cuprates, the inverse of g/g_c in Fig. 1 can be loosely associated with hole concentration [14]. Of importance for the cuprates is the prediction that the effective inverse lifetime in the electronic self-energy γ , which can be deduced experimentally [15], varies continuously to zero at T_c . Finally changes in our results associated with the *d*-wave, layered structure of the high T_c systems can be anticipated: the nodal structure of *d*-wave pairs will weaken the gap in the T-matrix which played an important role in determining the detailed temperature evolution of $\Delta_{\text{pg}}(T)$ and $\gamma(T)$ above T_c . Moreover, quasi-two dimensionality will considerably lower the energy scales and enhance the pseudogap regime, particularly as the insulator is approached. Despite these omissions, our physical picture of the interplay of the pseudogap and superconducting instability is expected to be qualitatively general, within a precursor superconductivity scenario.

We would like to thank A. Abanov, I. Kosztin, M. Norman and Y. Vilk for useful discussions. This research was supported in part by the Natural Sciences and Research Council of Canada (J.M.) and the Science and Technol-

ogy Center for Superconductivity funded by the National Science Foundation under award No. DMR 91-20000.

- [1] P. W. Anderson, *The Theory of Superconductivity in the High-Tc Cuprate Superconductors* (Princeton University Press, Princeton, 1997).
- [2] A. V. Chubukov *et al.*, J. Phys. (Cond. Matt.) **8**, 10017 (1996); J. R. Schrieffer and A. P. Kampf, J. Phys. Chem. Sol. **56**, 1673 (1995).
- [3] R. Klemm, (unpublished).
- [4] See, for example, K. Levin *et al.*, Phys. Rev. B **10**, 3821 (1974).
- [5] A. J. Leggett, J. Phys. (Paris) **41**, C7 (1980); P. Nozières and S. Schmitt-Rink, J. Low Temp. Phys. **59**, 195 (1985).
- [6] M. Randeria *et al.*, Phys. Rev. Lett. **62**, 981 (1989); C. A. R. Sa de Melo *et al.*, Phys. Rev. Lett. **71**, 3202 (1993).
- [7] N. Trivedi, and M. Randeria, Phys. Rev. Lett. **75**, 312 (1995).
- [8] B. Janko, J. Maly and K. Levin, Phys. Rev. B **56**, (to be published).
- [9] While we consider the *s*-wave symmetry case, *d*-wave symmetry can be readily introduced via the $\varphi_{\mathbf{k}}$.
- [10] B. R. Patton, PhD Thesis, Cornell University, 1971 (unpublished).
- [11] L. P. Kadanoff and P. C. Martin, Phys. Rev. **124**, 670 (1961); A. Klein, Nuovo Cimento **25**, 788 (1962).
- [12] M. Drechsler and W. Zwirger, Ann. Physik **1**, 15 (1992); C. A. R. Sa de Melo, M. Randeria, and J. R. Engelbrecht, Phys. Rev. Lett. **71**, 3202 (1993).
- [13] A zero range interaction was studied by R. Haussmann, Phys. Rev. B **49**, 12975 (1994), where a monotonic T_c curve was obtained from a scheme which involved dressing all Green's functions.
- [14] g_c is expected to decrease as the insulator is approached as a consequence of a three to two dimensional cross-over, as well as a reduction in the plasma frequency – see J. Maly, K. Levin, and D.Z. Liu, Phys. Rev. B **54**, 15657 (1996).
- [15] M. Norman, (unpublished).

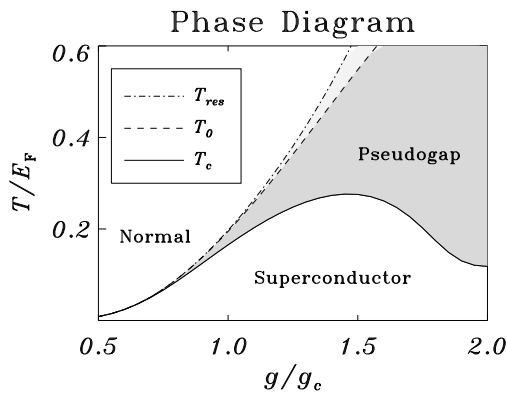


FIG. 1. Pseudogap phase diagram, which indicates the Fermi liquid breakdown co-responding to pair resonance onset, at T_{Res} , the fully self-consistent T_c and the transition temperature T_0 in the absence of mode coupling.

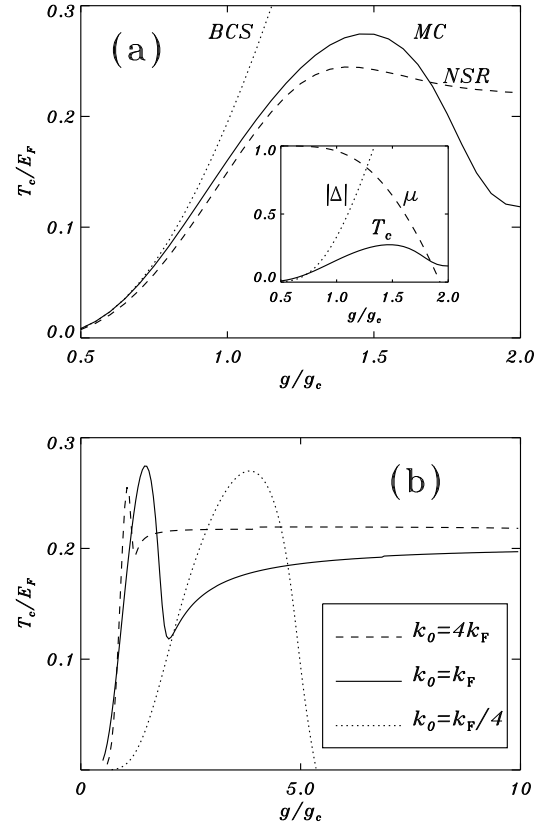


FIG. 2. (a) Comparison of the T_c curves in BCS theory, the Gaussian approximation of Nozières and Schmitt-Rink (NSR), and our mode coupling theory (MC). The inset plots the corresponding values of μ , Δ_{pg} , at T_c . (b) Variation of T_c for three different pairing interaction ranges.

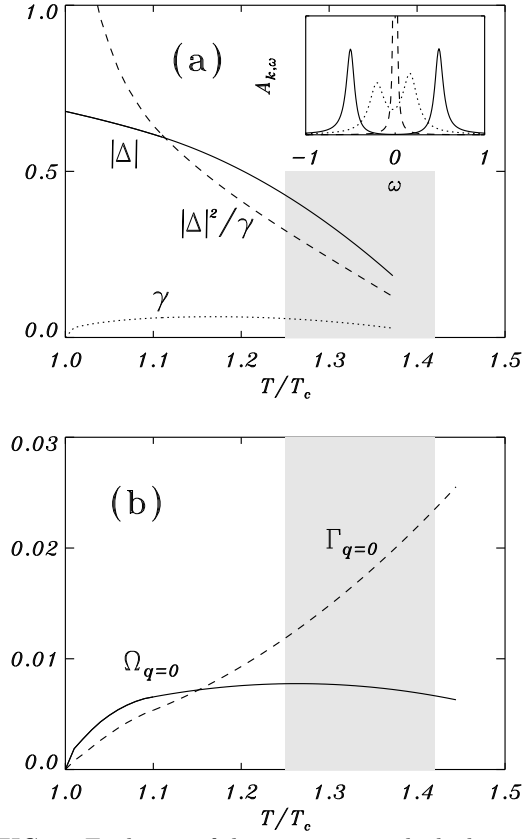


FIG. 3. Evolution of the parameters which characterize the electronic self-energy of Eq. 11, (a), and the pairing resonance (b). Shaded region represents the breakdown of Eq. 11 as well as lowest order theory. The latter is valid to right of shaded region. The values of Δ_{pg}^2/γ were divided by a factor of 10 and $g/g_c = 1.2$. Spectral functions are plotted in the inset, for the three temperature regimes.